THE JOURNAL OF PHYSICAL CHEMISTRY A

ARTICLE

pubs.acs.org/JPCA

Scattering of Xe from Graphite

W. W. Hayes*

Physical Sciences Department, Greenville Technical College, Greenville, South Carolina 29606, United States
Department of Physics and Astronomy, Clemson University, Clemson, South Carolina 29634, United States

J. R. Manson*

Department of Physics and Astronomy, Clemson University, Clemson, South Carolina 29634, United States

ABSTRACT: Recently a series of experimental measurements for the scattering of Xe atoms from graphite has been reported for both energy-resolved spectra and angular distributions. This system is of fundamental interest because the projectile Xe atoms are considerably more massive than the carbon atoms making up the graphite surface. These measurements were initially analyzed using the hard cubes model and molecular dynamics simulations, and both treatments indicated that the scattering process was a single collision in which the incoming Xe atom interacted strongly with a large number of carbon atoms in the outermost graphite layer. In this work we analyze the data using a single scattering theory that has been shown to explain a number of other experiments on molecular beam scattering from surfaces. These calculations confirm that the scattering process is a single collision with an effective surface mass that is substantially larger than that of the basic graphite ring.

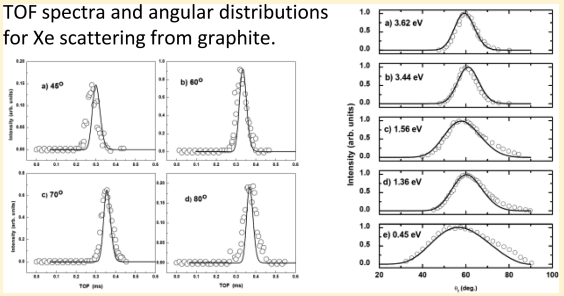

I. INTRODUCTION

An interesting and important series of measurements of the scattering of Xe atoms from a clean and ordered graphite (0001) surface has recently been reported.[1,2] These experiments present both energy-resolved spectra taken at fixed incident and detector angles and angular distributions in which the total in-plane scattered intensity is measured for a fixed incident angle as a function of final scattering angle. The authors analyzed their data using both the hard cubes model of scattering[3,4] and a molecular dynamics treatment that used Lennard-Jones interaction potentials. Both methods of analysis indicated that the scattering mechanism consisted of a single collision of the Xe projectile with the surface and that the Xe interacted strongly with a collective group of carbon atoms with a total mass of over 300 au. The molecular dynamics calculations showed that there was considerable deformation of the outermost graphite plane during the collision, but the strong intraplanar forces prevented the large and massive Xe atoms from penetrating through the outer layer. Because of this strongly collective and strongly repulsive motion of the outermost graphite layer, the authors gave it the name of a trampoline mechanism.

The objective of this work is to analyze this same data with a model of single collision scattering that has been successful for a number of other systems involving molecular beam scattering from surfaces. The theory is based on the classical mechanical model for surface scattering developed by Brako and Newns[5] with a scattering form factor for a hard repulsive interaction potential.[6,7] This theory has proven to be useful in explaining the energy-resolved spectra and angular distributions of rare gas atoms scattering from molten metal surfaces[8] and has also been useful in describing He and Ar scattering from graphene and C_{60} layers on a Pt(111) substrate.[9] Extensions of this theory to molecular scattering from surfaces have also been reported.[10] Thus it is of interest to investigate how this theoretical model can describe the scattering of the heavier projectile Xe from graphite.

The calculations with this model explain both the lineshapes and incident energy behavior of the data, but only upon assuming an effective surface mass that is considerably larger than the mass of a single carbon atom. This is in contrast to the results for scattering of rare gas atoms from low temperature melting point molten metals for which the effective mass was found to be equal to the metal atom mass for In and Bi and only slightly larger for Ga, where it was 1.65 times the Ga atomic mass. The effective mass ranged from 2.4 times the mass of a six-atom graphite ring (173 amu) at the lowest incident Xe atom energies of 0.45 eV to that of 4.2 graphite rings (302 amu) at the largest measured incident energy of 3.62 eV. These effective masses are comparable to or somewhat smaller than those found earlier[2] and confirm the conclusion that the collision process mechanism is primarily a single collision involving a large number of carbon atoms with no penetration beyond the first graphite layer.

Special Issue: J. Peter Toennies Festschrift

Received: November 22, 2010
Revised: January 21, 2011
Published: March 16, 2011

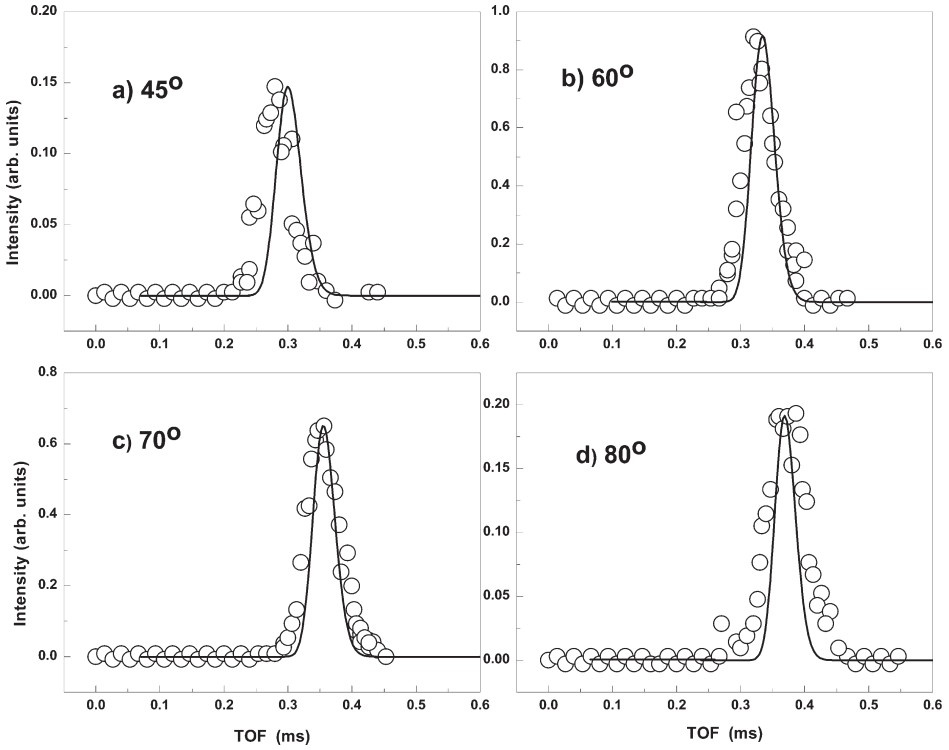

Figure 1. Reflected intensity as a function of TOF for Xe scattering from graphite. The incident angle is $\theta_i = 35°$, the incident energy is $E_i = 1.56$ eV and the surface temperature is $T_S = 550$ *K*: (a) final angle $\theta_f = 45°$, (b) final angle $\theta_f = 60°$, (c) final angle $\theta_f = 70°$, and (d) final angle $\theta_f = 80°$. Data points are from ref 1, and the present calculations are shown as a solid curve, with an effective surface mass equivalent to 3.8 graphite rings.

II. THEORY

The theoretical model used here is most readily described in terms of a differential reflection coefficient, $dR(\mathbf{p}_f,\mathbf{p}_i)/d\Omega_f\,dE_f$, giving the probability of an incident beam of particles with momentum $\mathbf{p}_i$ being scattered into a final energy dE_f and solid angle $d\Omega_f$ intervals centered about momentum $\mathbf{p}_f$[5,11,12]

$$\frac{dR(\mathbf{p}_f,\mathbf{p}_i)}{d\Omega_f dE_f} = \frac{m^2 v_R^2 |\mathbf{p}_f|}{8\pi^3\hbar^2 p_{iz} S_{uc}} |\tau_{fi}|^2 \left(\frac{\pi}{k_B T_S \Delta E_0}\right)^{3/2} \times \exp\left\{-\frac{(E_f - E_i + \Delta E_0)^2 + 2v_R^2 \mathbf{P}^2}{4k_B T_S \Delta E_0}\right\} \quad (1)$$

where m is the projectile atomic mass, p_{iz} is the surface-normal component of the incident momentum, T_S is the temperature, k_B is Boltzmann's constant, the binary recoil energy is $\Delta E_0 = (\mathbf{p}_f - \mathbf{p}_i)^2/2M_C$, with M_C being the effective surface mass, $\mathbf{P}$ is the parallel component of the scattering vector $\mathbf{p}_f - \mathbf{p}_i$, and $|\tau_{fi}|^2$ is a form-factor determined by the interaction potential. The factor S_{uc} is the unit cell area associated with a single surface atom and v_R is a parameter having dimensions of speed that is completely determined by the phonon spectral density at the surface. In a classical mechanical derivation of eq 1, the quantity $\hbar$ is a constant having dimensions of action, but a derivation starting from quantum mechanics and then taking the classical limit identifies this quantity as Planck's constant divided by 2π.

Consistent with the classical limit of a quantum mechanical derivation used to obtain eq 1, the form factor $|\tau_{fi}|^2$ is the transition matrix element for the elastic interaction potential extended off the energy shell. If the repulsive part of the interaction potential is flat and strongly repulsive, then the leading term in the perturbation series for the matrix element is

$$\tau_{fi} = 4p_{fz}p_{iz}/m \quad (2)$$

a limiting form that has been shown to be useful in other studies of atomic and molecular scattering from surfaces.[6,10]

For experiments such as the ones considered here, typically the detector is energy dependent, meaning that the probably of detection of a scattered atom is proportional to the time spent in the detector. This implies that for direct comparison with energy-resolved data the differential reflection coefficient must be corrected for the detector efficiency with a multiplicative factor proportional to this time, which is also proportional to the inverse of the final particle momentum.

III. CALCULATIONS

In Figure 1, calculations are shown compared with four examples of energy-resolved scattering spectra with data extracted from ref 1. The relative scattered intensity is plotted as a function of the time-of-flight (TOF) between the target crystal and the detector. The incident angle is 35° with respect to the surface normal and the final angles range from 45° to 80° in the opposite quadrant, and all measurements were taken in the scattering plane defined by the incident beam and the surface normal. The incident energy was 1.56 eV and the surface temperature was 550 K. The calculations shown as a solid curve were carried out with eq 1 and then converted to a TOF scale. The value of the effective surface mass is taken to be 3.8 graphite rings (273.6 amu) and v_R is 3000 m/s for all calculations reported here.

dx.doi.org/10.1021/jp111153q |*J. Phys. Chem. A* 2011, 115, 6838–6842

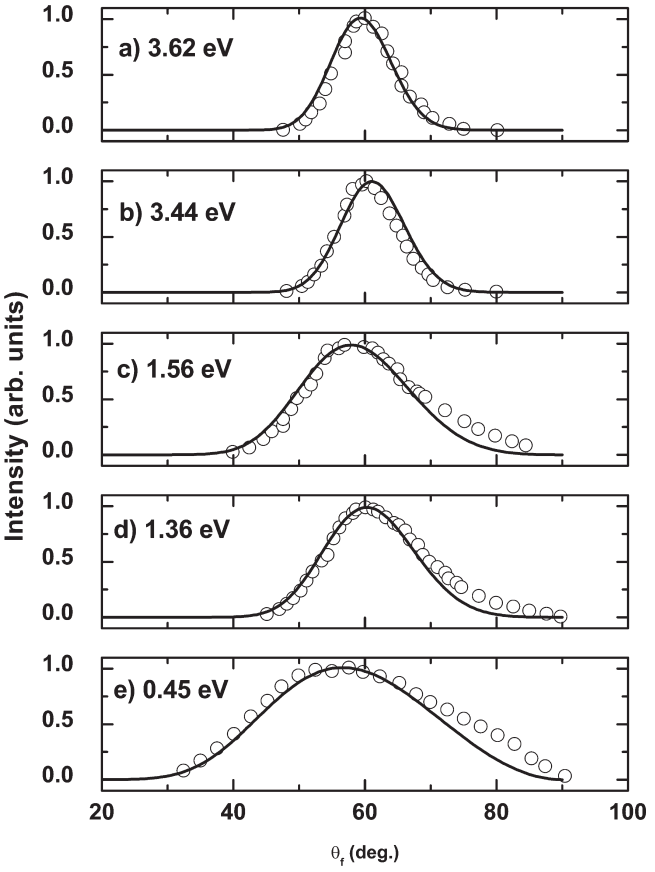

Figure 2. In-plane angular distributions for Xe scattering from graphite. The incident angle is $\theta_i = 35°$. Data points are from refs 1 and 2, and the present calculations are shown as solid curves with the effective mass m_{eff} given as the number of graphite rings. (a) $T_S = 550$ K, $E_i = 3.62$ eV, and $m_{eff} = 4.2$; (b) $T_S = 300$ K, $E_i = 3.44$ eV, and $m_{eff} = 3.9$; (c) $T_S = 550$ K, $E_i = 1.56$ eV, and $m_{eff} = 3.8$; (d) $T_S = 300$ K, $E_i = 1.36$ eV, and $m_{eff} = 3.7$; and (e) $T_S = 550$ K, $E_i = 0.45$ eV, and $m_{eff} = 2.4$.

The data exhibit a single narrow peak at a TOF corresponding to a typical total translational energy loss of more than 50% of the incident energy. The width of the peak does not change appreciably with final angle, but there is a pronounced energy shift toward longer flight times (smaller final energy) as the final detector angle is increased. Both the shape of the peak and the shift in energy with final angle are reasonably well reproduced by the calculations. The calculations are relatively insensitive to the value of the parameter v_R, but are quite sensitive to the effective surface mass and for smaller values of this mass the total energy loss becomes larger.

Figure 2 shows five examples of in-plane angular distributions each taken with a fixed incident angle of $\theta_i = 35°$ in which the relative intensity is plotted as a function of final detector angle. The incident translational energies range from 0.45 to 3.62 eV and the surface temperatures are either 300 or 550 K as noted. The data points are extracted from refs 1 and 2. The angular distributions consist of a single broad peak whose most notable behavior is a a strong narrowing of the full width at half-maximum (fwhm) with increasing energy, a characteristic of a single scattering mechanism.

The calculations are shown as solid curves, and are obtained from the integral of the differential reflection coefficient of eq 1 over all final energies after first accounting for the detector correction. In order to fit the calculations to the data, it was necessary to allow the effective surface mass to increase with incident energy, as was also found in the analyses of refs 1 and 2. As shown in Figure 2, the effective mass increases from that of 2.4 graphite rings (172.8 amu) at the lowest energy of 0.45 eV up to 4.2 graphite rings (302.4 amu) at the highest energy of 3.62 eV. Even with a constant effective mass, the calculations exhibit a significant narrowing of the fwhm with increasing energy, and in fact previously reported results for Ar scattering from graphite were well explained by a constant effective mass.[9] However, for the present case of Xe projectiles, the effective mass must be allowed to increase with incident energy in order to obtain agreement with the measurements. It is noticed that there is some small disagreement at larger final angles for the three lowest incident energies presented in Figure 2, with the experimental data exhibiting larger intensity than that predicted by the calculations. It has been suggested that this enhanced intensity observed in the data at supraspecular angles may be due to defects and impurities on the surface.[13]

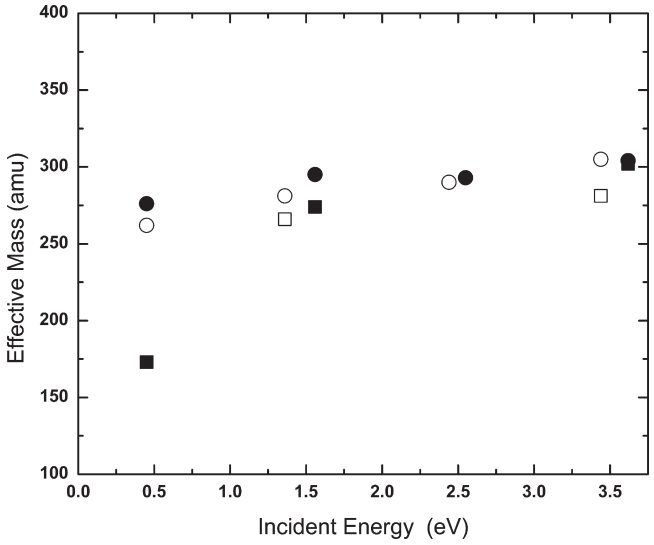

Figure 3. Effective mass of the graphite surface as a function of incident Xe energy. Filled and open circles are values for surface temperatures of 550 and 300 K, respectively, obtained by Shobatake et al.[2] The filled and open squares are the corresponding values obtained from the present calculations.

The evolution of the effective mass as a function of surface temperature and incident Xe energy is shown in Figure 3. The data points shown as circles give the effective masses obtained in ref 2 from an analysis of the angular distribution data for $\theta_i = 35°$ using the hard cubes model, with filled circles taken at a surface temperature $T_S = 550$ K and open circles at $T_S = 300$ K. The effective masses obtained from the present calculations are shown as filled and open square points for $T_S = 550$ and 300 K, respectively. The present calculations are not shown for the two experimental points at energies near 2.5 eV because the corresponding angular distributions were not published. There is a clear trend of increasing effective masses with increasing energies, and the present calculations give values that are of the same order or slightly smaller than those obtained previously using the hard cubes analysis, except for the very lowest energy where the present analysis predicts a substantially smaller mass.

IV. DISCUSSION AND CONCLUSIONS

This paper presents a new theoretical analysis of recently published scattering data for a beam of Xe atoms interacting with a graphite (0001) surface. This system is of particular interest

because of the large mass ratio between the projectile Xe atoms and the C atoms of the graphite target. Although other atom−surface scattering experiments have been carried out with Xe projectiles, the targets have usually been metals whose atoms are more massive than Xe.[14,15] A binary collision model with a single Xe atom colliding with a single C atom, or even a small cluster of C atoms would predict that the Xe atoms would follow a forward trajectory, which would imply penetration into the bulk. However, the energy-resolved TOF measurements show a single, relatively narrow peak in the scattered distribution at an energy loss of more than half of the incident energy. The angular distributions show a single broad peak at angles greater than the specular angle, and this peak has a fwhm that becomes smaller with increasing incident energy. These properties are indicative of a single collision, direct scattering mechanism.

As originally published, the data was analyzed in two ways, using the hard cubes model and a molecular dynamics treatment with Lennard-Jones interaction potentials.[1,2] The major conclusions were that the scattering mechanism was a single collision with the outermost layer of graphite and no penetration of the Xe atoms into the bulk. The use of the hard cubes model, which assumes that the collision is with a perpendicularly vibrating mass and allows for no energy exchange in the directions parallel to the surface, indicated that the energy transfer was primarily due to changes in the perpendicular momentum. The effective mass of the hard cube had to be substantially larger than that of a carbon atom, up to over 300 amu, which was indicative of the Xe atoms interacting with a large number of carbon atoms during the collision. The molecular dynamics simulations appeared to confirm this picture and indicated that the strong intraplanar forces in the graphite layer constrained the Xe and did not permit penetration, but caused substantial deformation involving a large number of carbon atoms, hence a large effective mass. The authors called this the trampoline model, since the outermost graphite layer of strongly linked carbon atoms flexes like a large sheet under collision with the Xe projectile.[1] In order for the hard cubes analysis to explain the data, the effective mass had to be increased with increasing incident energy, implying participation of a greater number of surface carbon atoms with larger energy.

This paper treats the same data with a somewhat different approach, a fully three-dimensional theory appropriate for a surface that is flat except for time-dependent thermal displacements due to the vibrations of the underlying surface atoms. This theory has been successful in explaining the energy-resolved and angular distribution scattering data for a number of other systems, including a recent treatment of scattering of He and Ar atoms from graphite.[9] The calculations do a good job of explaining both the measured energy-resolved TOF spectra and the angular distributions. As opposed to earlier treatments of scattering of rare gases from molten metal surfaces, the present analysis required the use of an effective mass much larger than that of a single carbon atom, in agreement with the original conclusions from the hard cubes analysis. With the use of a large effective mass, the present calculations correctly predict the energy losses observed in the TOF measurements, and correctly predict the positions, line shapes, and narrowing with energy of the angular distributions. The energy loss is found to be primarily due to the large change in normal momentum, i.e., the energy loss is predominantly associated with motion in the normal direction. The good agreement with all of these aspects of the data confirms the original conclusion that the scattering process is a single collision involving a large number of C atoms.

It is interesting to note that the present analysis, as well as the original analysis using the hard cubes model,[1,2] obtains reasonable agreement with the data under the assumption that the surface has no static corrugation. This appears to imply that corrugation at the length scale of the displacement between carbon atoms is relatively unimportant in causing the angular width of the observed angular distributions, a view that is consistent with a large number of carbon atoms being involved in the collision. The authors have recently developed an extension of the classical theory used here that includes surface corrugation,[16] and preliminary calculations seem to confirm that the corrugation plays a relatively small role in forming the shape of the angular distributions.

The effective mass necessary to obtain good agreement with the angular distribution data increases slightly with incident Xe atom energy, a fact that was also observed from the hard cubes model analysis.[1,2] This is interpreted as a consequence of the strong intraplanar forces in a graphene layer; with higher collision energy, a larger area of the graphene layer is deformed leading to more and more of the carbon atoms involved in the collision, hence a larger effective surface mass. For a given energy, the effective mass obtained in the present calculations tends to be slightly smaller than that resulting from the hard cubes model analysis. In both cases, the effective masses were primarily obtained from analysis of the angular distributions. The angular distributions, since they are a summation over all final energies at each final angle, necessarily contain less information about the scattering process than the energy resolved spectra at a given final angle. In the present analysis, the four available energy-resolved TOF spectra are reasonably well explained with the same effective mass as was derived from the angular distribution for the same incident angle and energy. Clearly, it would be of great interest to have a much larger collection of energy resolved TOF spectra for a wide range of incident angles and energies and final angles. Such measurements, when compared with theoretical calculations, would provide a much clearer picture of the effective mass and consequently the collective many-body nature of the collision process.

AUTHOR INFORMATION

Corresponding Author

*Electronic address: Wayne.Hayes@gvltec.edu; jmanson@clemson.edu.

ACKNOWLEDGMENT

The authors would like to thank T. Kondo for discussions and a critical reading of this manuscript.

REFERENCES

(1) Watanabe, Y.; Yamaguchi, H.; Hashinokuchi, M.; Sawabe, K.; Maruyama, S.; Matsumoto, Y.; Shobatake, K. *Chem. Phys. Lett.* **2005**, *413*, 331.

(2) Watanabe, Y.; Yamaguchi, h.; Hashinokuchi, M.; Sawabe, K.; Maruyama, S.; Matsumoto, Y.; Shobatake, K. *Eur. Phys. J. D* **2006**, *38*, 103.

(3) Logan, R. M.; Stickney, R. E. *J. Chem. Phys.* **1966**, *44*, 195.

(4) Logan, R. M.; Keck, J. C.; Stickney, R. E. *Rarefied Gas Dyn., 4th Symp.* **1967**, *5*, 49.

(5) Brako, R.; Newns, D. M. *Phys. Rev. Lett.* **1982**, *48*, 1859. Brako, R.; Newns, D. M. *Surf. Sci.* **1982**, *117*, 422.

(6) Andre Muis; Manson, J. R. *J. Chem. Phys.* **1997**, *107*, 1655.

(7) Muis, A.; Manson, J. R. *J. Chem. Phys.* **1999**, *111*, 730.
(8) Hayes, W. W.; Manson, J. R. *J. Chem. Phys.* **2007**, *127*, 164714.
(9) Yamada, Y.; Sugawara, C.; Satake, Y.; Yokoyama, Y.; Okada, R.; Nakayama, T.; Sasaki, M.; Kondo, T.; Oh, J.; Nakamura, J.; Hayes, W. W. *J. Phys.: Condens. Matter* **2010**, *22*, 304010.
(10) Ileana Iftimia; Manson, J. R. *Phys. Rev. Lett.* **2001**, *87*, 093201.
(11) Meyer, H.-D.; Levine, R. D. *Chem. Phys.* **1984**, *85*, 189.
(12) Manson, J. R. *Phys. Rev. B* **1991**, *43*, 6924.
(13) Oh, J.; Kondo, T.; Hatake, D.; Honma, Y.; Arakawa, K.; Machida, T.; Nakamura, J. *J. Phys.: Condens. Matter* **2010**, *22*, 304008.
(14) Hurst, J. E.; Becker, C. A.; Cowan, J. P.; Janda, K. C.; Wharton, L.; Auerbach, D. J. *Phys. Rev. Lett.* **1979**, *43*, 1175.
(15) Rettner, C. T.; Barker, J. A.; Bethune, D. S. *Phys. Rev. Lett.* **1991**, *67*, 2183.
(16) Hayes, W. W.; Manson, J. R. To be submitted for publication.